PERGAMON

Computerized Medical Imaging and Graphics 25 (2001) 97–103

Computerized Medical Imaging and Graphics

www.elsevier.com/locate/compmedimag

Image reconstruction — a tutorial

G.L. Zeng*

MIRL, 729 Arapeen Drive, University of Utah, Salt Lake City, UT 84108-1218, USA

Received 20 April 2000

Abstract

This paper is written for physicians and presents basic principles of image reconstruction in nuclear medicine. Both analytical and iterative methods are discussed without rigorous mathematics.

Keywords: Image reconstruction; Tomography; Reconstruction algorithms; Analytical reconstruction; Iterative reconstruction; Tutorial

1. Introduction

Suppose you are touring Belgium and you have discovered a unique example of architecture and you would like to share your experience with your friends back home. You take out your camera and take a picture of it. In order to get a better representation of the building, you decide to take more pictures of it from different angles. This principle applies in medical imaging, where an accurate internal image is obtained by combining pictures from different views.

In nuclear medicine, the single photon emission computed tomography (SPECT) or positron emission tomography (PET) camera rotates around the patient, taking pictures of radioisotope distribution within the patient from different angles. These "pictures" acquired from the nuclear medicine camera are called *projections*. The procedure to put the projections together to obtain a patient's image is called *image reconstruction*, as shown in Fig. 1.

In most cases, one of two types of algorithms is used in reconstructing images: analytical and iterative algorithms. An algorithm is a step-by-step mathematical procedure implemented on a computer. In nuclear medicine, image reconstruction is performed in a computer with reconstruction algorithms.

2. Analytical algorithms

2.1. Filtered backprojection algorithm

Let us consider a special situation in which the image is two-dimensional (2D) and it consists of only one point with a certain degree of intensity, as shown in Fig. 2(a), where the high of the "pole" indicates the intensity of the point in the object (image). A number of projections are taken from various angles as shown in Fig. 2(b). Assuming that you are at the point where you have obtained the projections but you have not assembled them into, how would you reconstruct the image using those projections? When you look at the projections, you see a spike. This spike is the sum of all activity along the projection path. To reconstruct the image, you must re-distribute the activity in the spike back to its original path. The problem is that you do not know where along the path you need to put more activity and where along the path you need to put less. Before you give up, you decide to put equal amounts of activity everywhere along the path, and the amount is the high of the projection spike. You do that for all of projections taken from every angle, as shown in Fig. 2(c). What you have just done is a standard mathematical procedure called *backprojection*. If you backproject from all angles over 360°, you will produce an image similar to the one shown in Fig. 2(d).

After backprojection, the image is not quite the same as the original image, but rather is a blurred version of it. In order to sharpen the image, we apply special "filtering" to the projections by introducing negative wings before backprojection. The use of the negative wings results in a clear image (see Fig. 3). This image reconstruction algorithm is very common and is referred to as a Filtered Backprojection Algorithm.

Fig. 4 shows a computer simulation that demonstrates the filtered backprojection algorithm in action. Fig. 4(a) shows the projection sinogram. A sinogram is a way to display the projections, where projection data at one view are put in one row of the sinogram and the vertical direction represents the view angle. A point in the image corresponds to a sine wave

* Tel.: +1-801-581-3918; fax: +1-801-585-3592.
E-mail address: larry@doug.med.utah.edu (G.L. Zeng).

0895-6111/01/$ - see front matter
PII: S0895-6111(00)00059-8

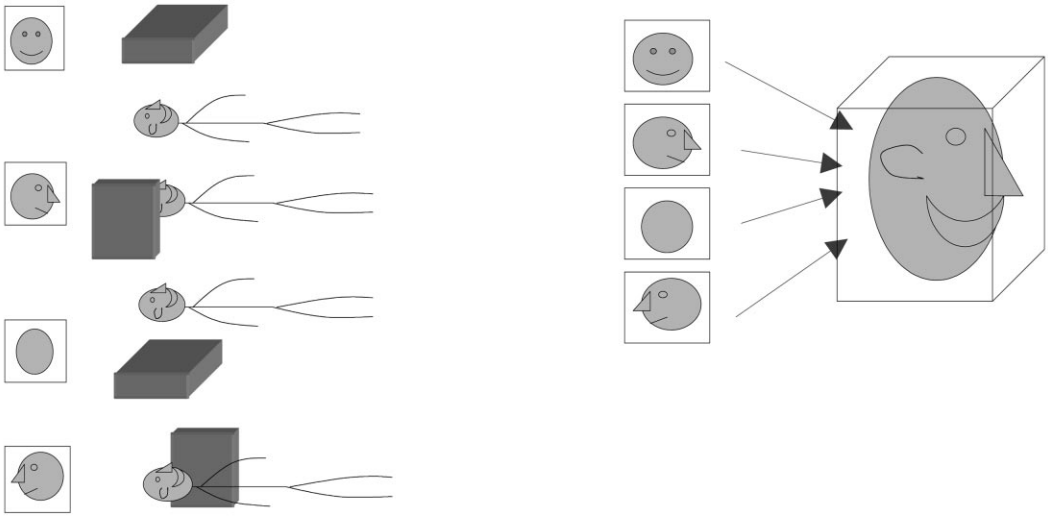

Fig. 1. Projection data acquired from different views are used to reconstruct the image.

in the sinogram. After the special filtering done by introducing negative wings, the sinogram shows two dark bands, which encapsulate each sine wave (see Fig. 4(b)). The backprojection step is shown in different stages in Fig. 4(c–h). A perfect image is reconstructed when the backprojection is performed over 180°.

2.2. Other analytical algorithms

In practice, when radiation photons travel through the patient's body before reaching the detector, the patient's body itself attenuates the photons. This attenuation effect can be handled by a filtered backprojection reconstruction algorithm if we assume that the attenuation is uniform within the patient.

In SPECT, the collimators cause distance-dependent blurring, which is shown in Fig. 5. When the object is farther away from the detector, the more severe the blurring becomes. In a filtered backprojection reconstruction algorithm this problem is handled by something called the *frequency–distance relationship*.

In both of the attenuation and distance-dependent blurring compensation cases presented above, the projection data are first pre-processed, then applied to the filtered backprojection algorithm. The pre-processing step involves a mathematical procedure called *Fourier transform* of the projection sinogram.

The Fourier transform decomposes an image into components, which are referred to as frequency components. To illustrate Fourier transform, let us look at the prism shown in Fig. 6, where incoming white light is decomposed into different colors (frequency components). The inverse procedure is to recombine the components into white light. The prism acts like a Fourier transform operator and the inverse procedure as an Inverse Fourier transform operator. One can manipulate the frequency components in the frequency space (i.e. where the white light is decomposed into different colors) as needed for different purposes.

In order to compensate for uniform attenuation, the projections are multiplied by an exponential function, which is determined by the object boundary, resulting in modified sinogram. Then, the Fourier transform of the modified sinogram is taken. From that the frequency components are re-mapped according to the attenuation coefficient. Following that the Inverse Fourier transform is taken and the filtered backprojection algorithm is used to reconstruct the image.

In order to compensate for distance-dependent system blurring, the Fourier transform of the projection data sinogram is taken, then the frequency components are filtered according to the frequency–distance principle, which relates the activity depth to certain frequency components. Following that the Inverse Fourier transform is taken and the filtered backprojection algorithm is used to reconstruct the image.

The filtered backprojection algorithms also exist for other imaging geometries, for example, the fan beam geometry as shown in Fig. 7.

There are other types of analytical algorithms in which the backprojection is performed first and filtering follows. These types of algorithms are called *Backprojection Filtering* algorithms.

2.3. Three-dimensional image reconstruction

A three-dimensional (3D) image can be formed by stacking slices of 2D images, as shown in Fig. 8. However, this approach does not always work. Figs. 9 and 10 show 3D PET and cone-beam imaging geometries, respectively. We observe from these figures that there are projection rays that cross multiple image slices. This makes slice-by-slice reconstruction impossible. Thus, truly 3D reconstruction is required.

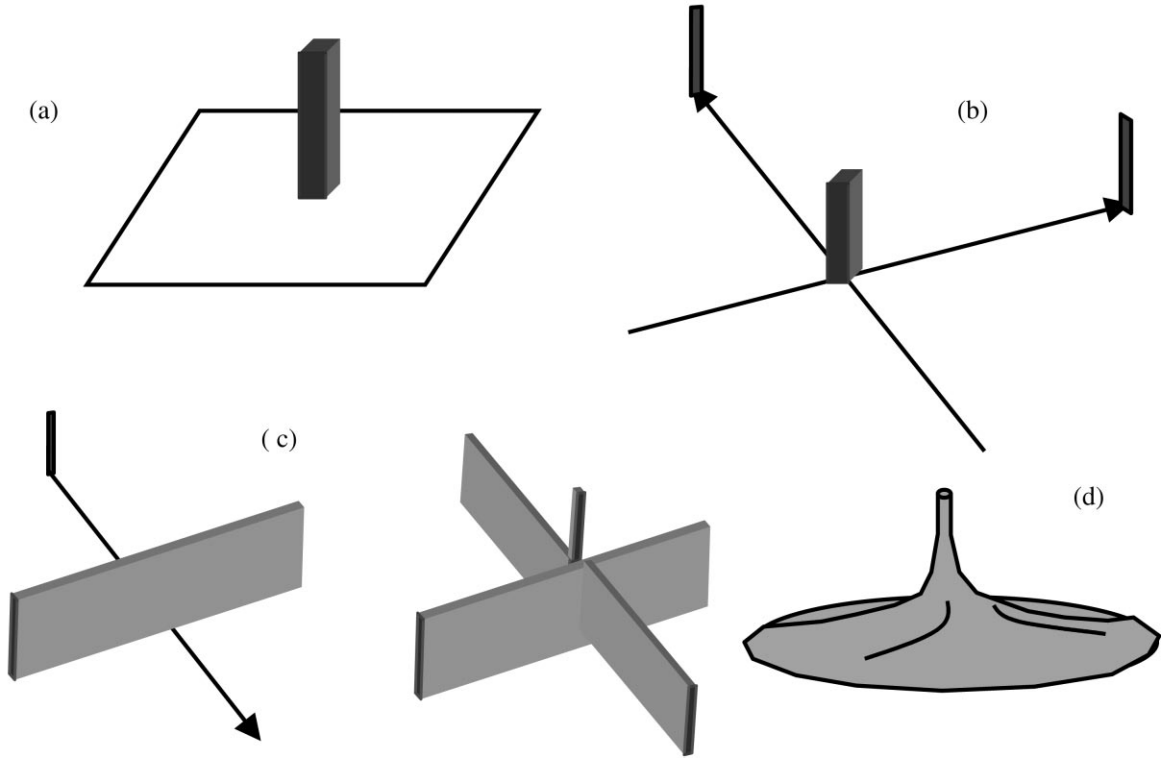

Fig. 2. Projection and backprojection.

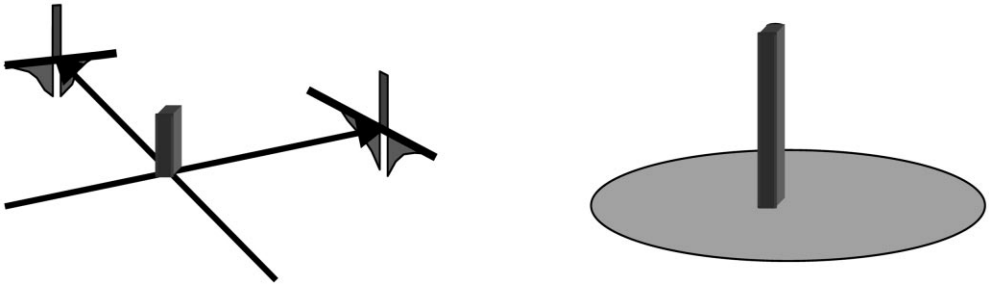

Fig. 3. In filtered backprojection, negative wings are introduced to eliminate blurring.

Both filtered backprojection and backprojection filtering algorithms exist for truly 3D reconstruction. Such algorithms require parallel plane (or line) measurements from various directions as shown in Fig. 11.

Recently, rebinning methods have been developed to convert 3D measurements with rays that traverse transaxial slices into "decomposed" measurements without those crossing rays, so that efficient slice-by-slice 2D reconstruction is possible.

3. Iterative reconstruction

In nuclear medicine, iterative reconstruction is becoming popular for the following reasons: (1) it is easy to model and handle projection noise, especially when the counts are low; and (2) it is easy to model the imaging physics, such as geometry, non-uniform attenuation, scatter, and so on.

The basic process of iterative reconstruction is to discretize the image into pixels and treat each pixel value as an unknown. Then a system of linear equations can be set up according to the imaging geometry and physics. Finally, the system of equations is solved by an iterative algorithm. The setup of equations is shown in Fig. 12. The system of linear equations can be represented in the matrix form as $\boldsymbol{FX} = \boldsymbol{P}$, where each element ($X_j$) in $\boldsymbol{X}$ is a pixel value, each element (P_i) in $\boldsymbol{P}$ is a projection measurement, and F_{ij} in $\boldsymbol{F}$ is a coefficient that is the contribution from pixel j to the projection bin i.

The diagram in Fig. 13 shows the basic procedure for using an iterative algorithm. Each loop in Fig. 13 represents

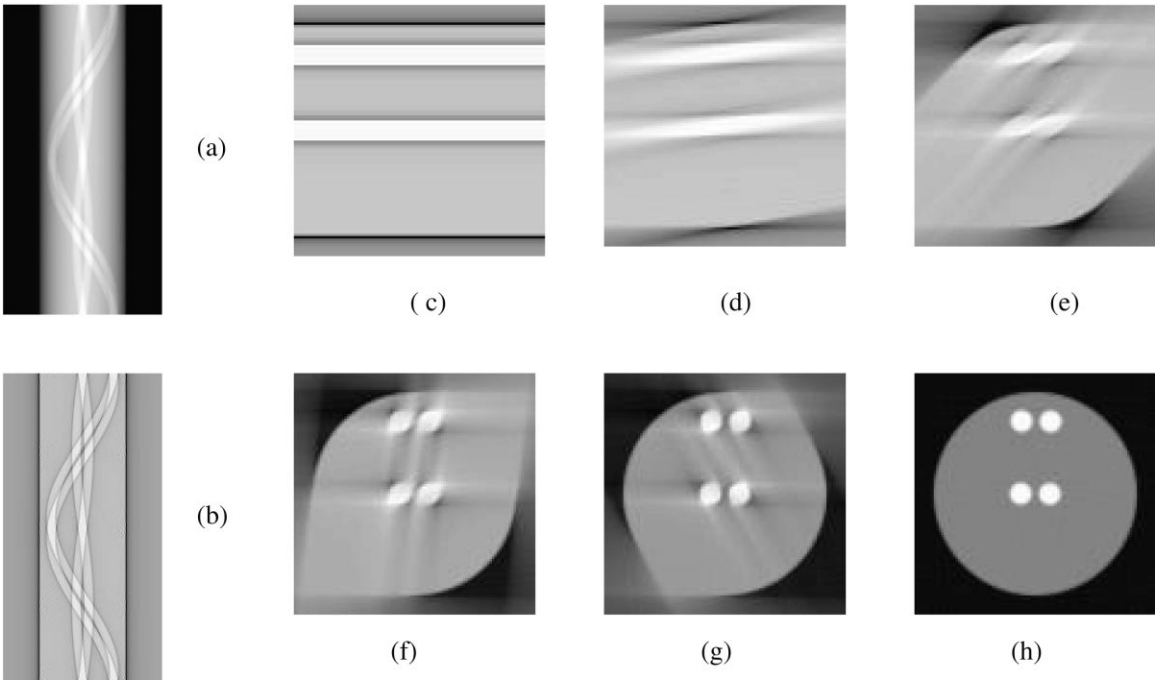

Fig. 4. A computer simulation of a filtered backprojection reconstruction.

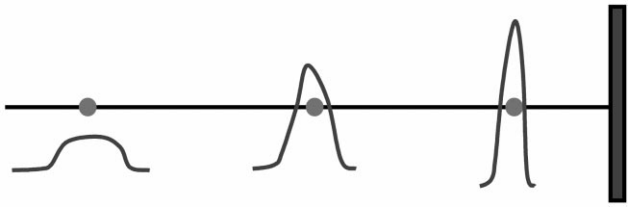

Fig. 5. Image blurring worsens the farther an object is away from the detector.

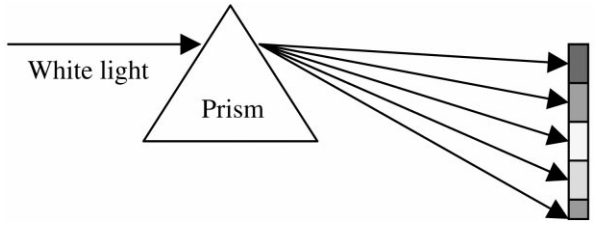

Fig. 6. Illustration of Fourier transform. A prism splits white light and transforms it into different colors.

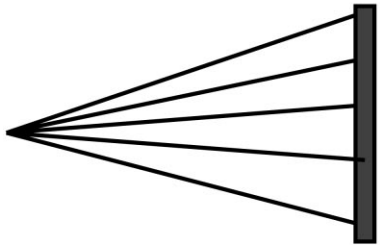

Fig. 7. An example of non-parallel beak imaging geometry.

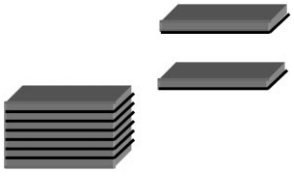

Fig. 8. In many cases, a 3D image can be reconstructed by stacking 2D reconstructions.

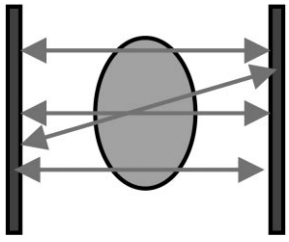

Fig. 9. In 3D PET, projection rays that cross slices are used.

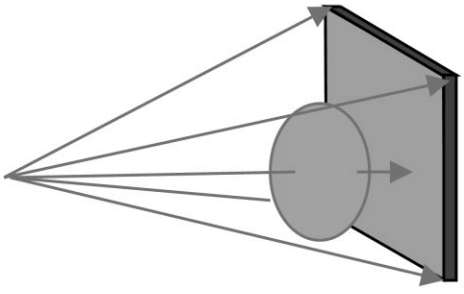

Fig. 10. A cone-beam imaging geometry.

Fig. 11. Parallel plane measurements in 3D.

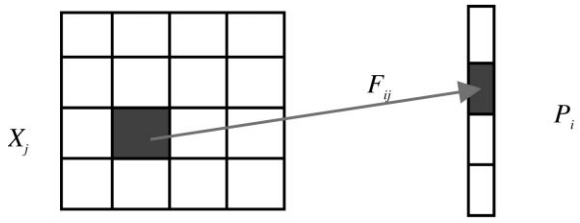

Fig. 12. The image is discretized into pixels and a system of equations is set up to describe the imaging geometry and physics.

one iteration. The initial estimate of the image in an iterative algorithm is usually a constant. Fig. 14 shows a computer simulation that demonstrates an iterative algorithm in action. In this simulation, the projection data contain noise. As the iterative procedure progresses, the reconstruction first converges to a recognizable image and then "diverges" to noise. This illustrates the importance of noise regularization in an iterative algorithm. The simplest method for regularization is to stop the iteration at a certain point.

Iterative reconstruction algorithms have several advantages over analytical reconstruction algorithms, because many imaging physics, such as non-uniform attenuation and scatter, can be modeled in the matrix **F**, whereas they are difficult to handle in an analytic algorithm. The most frequently used iterative algorithm in nuclear medicine applications is the ML-EM (maximum likelihood expectation maximization) algorithm. The ML-EM algorithm solves a set of linear equations, assuming Poisson noise is present in the projection data. A unique property of the ML-EM algorithm is that it produces an image with non-negative pixel values.

4. Summary

Analytic reconstruction algorithms, for example the filtered backprojection algorithm, are efficient and elegant, but they are unable to handle complicated factors such as scatter. Iterative reconstruction algorithms on the other hand are more versatile but less efficient. Efficient (i.e. fast) iterative algorithms are currently under development. With rapid increases being made in computer speed and memory, iterative reconstruction algorithms will be used in more and more applications and will enable more quantitative reconstructions.

This tutorial article describes basic principles of image reconstruction in nuclear medicine. An intuitive approach is adopted to explain the components in both analytical and iterative algorithms. In analytical algorithms, the filtered backprojection method is emphasized. Constant attenuation correction and distance-dependent blurring correction are briefly mentioned. The iterative reconstruction scheme is illustrated with a flow-chart. A list of references [1–54] is provided for those readers with further interest in the development of image reconstruction.

Acknowledgements

The author thanks Sean Webb for editorial assistance.

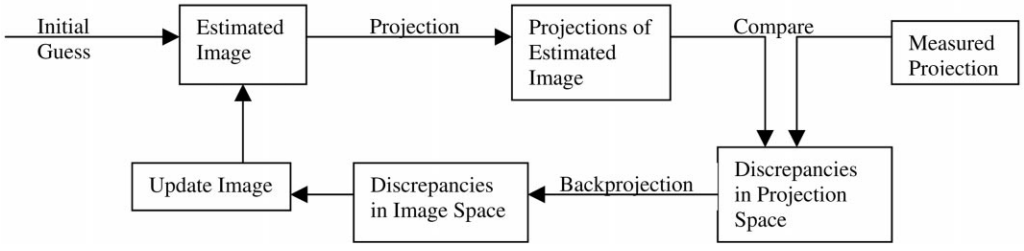

Fig. 13. Flow chart of iterative image reconstruction scheme.

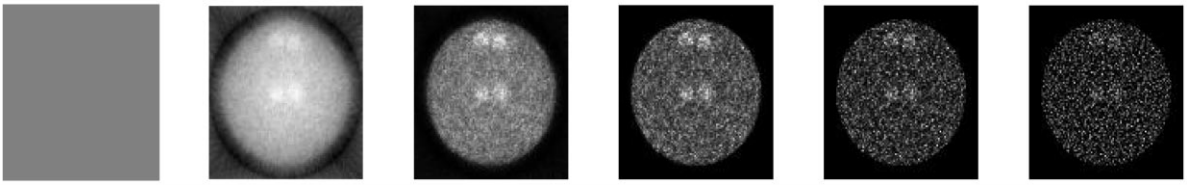

Fig. 14. An example of iterative reconstruction. From left to right, the iteration number is increased in each image.

References

[1] Kak AC, Slaney M. Principles of computerized tomographic imaging. New York: IEEE Press, 1988.

[2] Macovski A. Medical imaging systems. Englewood Cliffs, NJ: Prentice-Hall, 1983.

[3] Herman GT. Image reconstruction from projections: the fundamentals of computerized tomography. New York: Academic Press, 1980.

[4] Deans SR. The radon transform and some of its applications. New York: Wiley, 1983.

[5] Bracewell RN. Two-dimensional imaging. Englewood Cliffs, NJ: Prentice-Hall, 1995.

[6] Natterer N. The mathematics of computerized tomography. New York: Wiley, 1986.

[7] Barret HH, Swindell WE. Radiological imaging. New York: Wiley, 1980.

[8] Brooks RA, Di Chiro G. Principles of computer assisted tomography (CAT) in radiographic and radioisotopic imaging. Phys Med Biol 1976;21(5):689–732.

[9] Hawkins WG, Yang N-C, Leichner PK. Validation of the circular harmonic transform (CHT) algorithm for quantitative SPECT. J Nucl Med 1991;32:141–50.

[10] Lewitt RM, Edholm PR, Xia W. Fourier method for correction of depth-dependent collimator blurring, SPIE. Med Imag III: Image Process 1989;1092:232–43.

[11] Soares EJ, Byrne CL, Glick SJ, Appedorn CR, King MA. Implementation and evaluation of an analytical solution to the photon attenuation and non-stationary resolution reconstruction problem in SPECT. IEEE Trans Nucl Sci 1993;40:1231–7.

[12] Pan X, Metz CE. Non-iterative methods and their noise characteristics in 2D SPECT image reconstruction. IEEE Trans Nucl Sci 1997;44:1388–97.

[13] Inouye T, Kose K, Hasegawa A. Image reconstruction algorithm for single-photon-emission computed tomography with uniform attenuation. Phys Med Biol 1989;34:299–304.

[14] Bellini S, Piacenti M, Caffario C, Rocca F. Compensation of tissue absorption in emission tomography. IEEE Trans Acoust Speech, Signal Process 1979;ASSP-27:213–8.

[15] Gullberg GT, Budinger TF. The use of filtering methods to compensate for constant attenuation in single-photon emission computed tomography. IEEE Trans Biomed Engng 1981;28:142–57.

[16] Chen J. A theoretical framework of regional cone-beam tomography. IEEE Trans Med Imag 1992;11:342–50.

[17] Clack R. Overview of reconstruction algorithms for exact cone-beam tomography. SPIE Math Methods Med Imag III 1994;2299:230–41.

[18] Grangeat P. Analysis d'un système d'imagerie 3D par réconstruction à partir de radiographies X en géométrie conique, PhD thesis, l'Ecole Nationale Supérieure Des Télécommunications, 1987.

[19] Smith BD. Image reconstruction from cone-beam projections: necessary and sufficient conditions and reconstruction methods. IEEE Trans Med Imag 1985;MI-4:14–25.

[20] Tuy HK. An inversion formula for cone-beam reconstruction algorithm. SIAM J Appl Math 1983;43:546–52.

[21] Feldkamp LA, Davis LC, Kress JW. Practical cone-beam algorithm. J Opt Soc Am 1984;A1:612–9.

[22] Chui M-Y, Barrett HH, Simpson RG. Three-dimensional reconstruction from planar projections. J Opt Soc Am 1980;70:755–62.

[23] Cho ZH, Ra JB, Hilal SK. True three-dimensional reconstruction (TTR)-application of algorithm toward full utilization of oblique rays. IEEE Trans Med Imag 1983;MI-2:6–18.

[24] Cormack AM. Representation of a function by its line integrals, with some radiological applications. J Appl Phys 1963;34:2722–7.

[25] Orlov SS. Theory of three-dimensional reconstruction: II. The recovery operator. Sov Phys — Crystallogr 1975;20:701–9.

[26] Shepp LA, Logan BF. The Fourier reconstruction of a head section. IEEE Trans Nucl Sci 1974;21:21–43.

[27] Ramachandrn GN, Lakshminarayanan RV. Three-dimensional reconstruction from radiographs and electron micrographs: applications of convolutions instead of Fourier transforms. Proc Natl Acad Sci, USA 1971;68:2236–41.

[28] Basko RE, Zeng GL, Gullberg GT. Application of spherical harmonics to image reconstruction for the Compton camera. Phys Med Biol 1998;43:887–94.

[29] Budinger TF, Gullberg GT, Huesman RH. Emission computed tomography. In: Herman GT, editor. Image reconstruction from projections, Berlin: Springer, 1979. p. 147–246.

[30] Zeng GL, Hsieh Y-L, Gullberg GT, rotating A. and warping projector-backprojector pair for fan-beam and cone-beam iterative algorithms. IEEE Trans Nucl Sci 1994;41:2807–11.

[31] Liang Z, Jaszczak RJ, Turkington TG, Gilland DR, Coleman RE. Simultaneous compensation for attenuation, scatter, and detector response of SPECT reconstruction in three dimensions. Phys Med Biol 1992:587–603.

[32] McCarthy AW, Miller MI. Maximum likelihood SPECT in clinical computation times using mesh-connected parallel computers. IEEE Trans Med Imag 1991;10:426–36.

[33] Formiconi AR, Pupi A, Passeri A. Compensation of spatial system response in SPECT with conjugate gradient reconstruction technique. Phys Med Biol 1989;34:69–84.

[34] Liang Z, Turkington TG, Gilland DR, Jaszczak RJ, Coleman RE. Simultaneous compensation for attenuation, scatter and detector response for SPECT reconstruction in three dimensions. Phys Med Biol 1992;37:587–603.

[35] Riaku AT, Gortel AW. Photon propagation and detection in single-photon emission computed tomography — an analytic approach. Med Phys 1994;21:1311–21.

[36] Riaku AT, Hooper HR, Gortel ZW. Experimental and numerical investigation of the 3D SPECT photon detection kernel for non-uniform attenuating media. Phys Med Biol 1996;41:1167–90.

[37] Jaszczak RJ, Greer KL, Floyd CE, Harris CC, Coleman RE. Improved SPECT quantification using compensation for scattered photons. J Nucl Med 1984;25:893–900.

[38] Ogawa K, Harata Y, Ichihara T, Kubo A, Hashimoto S. A practical method for position-dependent Compton-scatter correction in SPECT. IEEE Trans Med Imag 1991;10:408–12.

[39] Gilland DR, Jaszczak RJ, Wang H, Turkington TG, Greer KL, Coleman RE. A.3D model of non-uniform attenuation and detector response compensation for efficient reconstruction in SPECT. Phys Med Biol 1994;39:547–61.

[40] Bowsher JE, Johnson VA, Turkington TG, Jaszczak RJ, Floyd CE, Coleman RE. Bayesian reconstruction and use of anatomical a priori information for emission tomography. IEEE Trans Med Imag 1996;15:673–86.

[41] Floyd CE, Jaszczak RJ, Coleman RE. Maximum likelihood reconstruction for SPECT with Monte Carlo modeling: Asymptotic behavior. IEEE Trans Nucl Sci 1987;34:285–7.

[42] Frey EC, Tsui BMW. Modeling the scatter response function in inhomogeneous scattering media for SPECT. IEEE Trans Nucl Sci 1994;41:1585–93.

[43] Welch A, Gullberg GT, Christian PE, Datz FL. A transmission-map-based scatter correction technique for SPECT in inhomogeneous media. Med Phys 1995;22:1627–35.

[44] Beekman FJ, Kamphuis C, Frey EC. Scatter compensation methods in 3D iterative SPECT reconstruction: a simulation study. Phys Med Biol 1997;42:1619–32.

[45] Tung C-H, Gullberg GT, Zeng GL, Christian PE, Datz FL, Morgan HT. Non-uniform attenuation correction using simultaneous transmission and emission converging tomography. IEEE Trans Nucl Sci 1992;39:1134–43.

[46] Liang Z, Jaszczak RJ, Floyd CE, Greer KL, Coleman RE. Reprojection and back projection in SPECT image reconstruction. Proc IEEE Energy Inform Technol Southeast 1989;EITS-1:919–26.

[47] McCarthy AW, Miller MI. Maximum likelihood SPECT in clinical

computation times using mesh-connected parallel computers. IEEE Trans Med Imag 1991;10:426–36.
[48] Zeng GL, Gullberg GT, Bai C, Christian PE, Trisjono F, DiBella EVR, Tanner JW, Morgan HT. Iterative reconstruction of Fluorine-18 SPECT Using geometric point response correction. J Nucl Med 1998;39:124–30.
[49] Wallis JW, Miller TR, Miller MM, Hamill J. Rapid 3-D projection in iterative reconstruction using Gaussian diffusion. J Nucl Med 1996;37:63 (abstract).
[50] Bowsher JE, Floyd CE. Treatment of Compton scattering in maximum-likelihood, expectation-maximization reconstructions of SPECT images. J Nucl Med 1991;32:1285–91.
[51] Lange K, Carson R. EM reconstruction algorithms for emission and transmission tomography. J Comput Assist Tomogr 1984;8:306–16.
[52] Hudsonand HM, Larkin RS. Accelerated EM reconstruction using ordered subsets of projection data. IEEE Trans Med Imag 1994;13:601–9.
[53] Byrne CL. Block-iterative methods for image reconstruction from projections. IEEE Trans Image Process 1996;5:792–4.
[54] Snyder DL, Schulz TJ, O'Sullivan JA. Deblurring subject to nonnegativity constraints. IEEE Trans Signal Process 1992;40(5):1143–50.

G. Larry Zeng obtained his PhD (1988) and a masters degree (1986) from the University of New Mexico, both in Electrical Engineering. His BS degree was in Applied Mathematics from Xidan University, China, in 1982. Dr Zeng is currently an Associate Professor in the Department of Radiology, the University of Utah. His research is to develop image reconstruction algorithms in single photon emission tomography (SPECT) and cone-beam imaging.